Radiocarbon, Vol 56, Nr 2, 2014, p 387–398 DOI: 10.2458/56.16944

^{14}C DATING AND MATERIAL ANALYSIS OF THE LIME BURIAL OF COVA DE NA DENT (MALLORCA, SPAIN)

Guy De Mulder[1] • Roald Hayen[2] • Mathieu Boudin[2] • Tess van den Brande[2] • Louise Decq[2] • Magdalena Salas Burguera[3] • Damià Ramis[4] • Herlinde Borms[5] • Mark Van Strydonck[2]

ABSTRACT. Lime burials are a characteristic phenomenon of the protohistoric funerary tradition on the Balearic Islands. At Cova de Na Dent, a lime burial has been sampled for analysis. The lime burial was made up of lime and fragmented bones. Six layers were sampled and described in the laboratory according to their color, the consistency of the deposition, and the aspect and quantity of the bone fragments. Bone samples and lime were dated. The lime was analyzed by using petrographic analysis, X-ray diffraction, FTIR spectroscopy, and simultaneous thermal analysis. The results show that the bones were cremated in the presence of crushed rock carbonate. The ^{14}C dates on the lime suggest an earlier chronology for this ritual, starting in the Bronze Age, as generally is accepted.

INTRODUCTION

The protohistoric "quicklime burials" from the Balearic Islands are a special type of cremation burial involving the transformation by heat of rock carbonate into quicklime (Van Strydonck et al. 2013). Probably before cremation the body was covered with a layer of fine crushed limestone. Until now, only museum samples, perhaps subject to unknown taphonomic processes since their excavation more than 20 yr ago, could be analyzed (Van Strydonck and Waldren 1990; Waldren and Van Strydonck 1995; Van Strydonck et al. 2011). This article discusses the results of samples analyzed within 1 yr after being excavated and stored in good conditions. The aims of this study are

1) To test if the apparent carbon exchange observed on the bone apatite from the museum collections could be verified on freshly excavated material and in this way overrule the possibility of a post-excavation phenomenon;

2) To establish an absolute date for the lime burial by dating the lime; and

3) To verify if the simultaneous thermal analysis (STA) can supply extra information on the amount of fossil carbonate still present in the lime.

The lime burial site of Cova de Na Dent (39°30′54.33″N, 3°18′19.92″E) is situated on Mallorca's west coast in the cliffs between S'Estany d'en Mas and Cala Falcó (Figure 1). The area is rich in karstic cave formations. Cova de Na Dent is situated in the Area Natural de Cales de Manacor in a cliff wall overlooking the sea (Figure 2).

SITE DESCRIPTION

At the southwestern entrance of the cave, a lime burial layer was preserved. The layer was still *in situ* but had been partly damaged due to illegal diggings. A section could be cleaned for the research purposes. This lime burial is about 40 cm thick, laying on undisturbed natural red-brownish clayey

---

1. Department of Archaeology, Ghent University, Sint-Pietersnieuwstraat 35, 9000 Ghent, Belgium.
2. Royal Institute for Cultural Heritage, Jubelpark 1, B-1000 Brussels, Belgium.
3. Museum of Manacor's History, Carretera Cales de Mallorca km. 1,5, 07500 Manacor, Balearic Islands, Spain.
4. Natural History Society of the Balearics, Margarida Xirgú 16, 07011 Palma de Mallorca, Balearic Islands, Spain.
5. Antwerp Society for Roman Archaeology (AVRA), Groenenborgerlaan 35, 2610 Wilrijk, Belgium.
Corresponding author. Email: Guy.DeMulder@UGent.be.

Proceedings of the Radiocarbon and Archaeology 7th International Symposium
Ghent, Belgium, April 2013 | Edited by Mark Van Strydonck, Philippe Crombé, and Guy De Mulder

Figure 1 Location of Cova de Na Dent

Figure 2 View of the cave; the burial was situated to the right of the person pictured

soil. The burial was covered with loose stone material. The lime was very hard and mixed with bone fragments. Individual burial depositions cannot be recognized within the lime conglomerate. No archaeological artifacts or charcoal were found in the lime burial except for a small fragment of a deteriorated bronze object, which could not be identified. In the laboratory, two very small fragments of iron were noticed; however, because of their size they were regarded as a postdepositional intrusion. During the cleaning of the area, a rim fragment of Islamic pottery was found, testifying to the later use of the cave.

The samples consisted of lumps made up of lime, bones, and powder. In general, the bones (Figure 4) changed from black and gray burned bones to very white and well-cremated remains. Several bones had a pale green color. This color seemingly comes from the copper in the bronze objects that must have been disposed with the bodies on the pyre. Samples have been taken at different levels and have been numbered from bottom (layer −1) to top (layer 3) for practical reasons since no visible structure in the lime burial was recognized. However, in the laboratory remarkable differences in the color of the lime (mixed with soil) were noticed due to the better lighting (see Figure 3). Based on the color, layer 2 was split into two sublayers: 2a and 2b.

Figure 3 Color differences of the lime between the layers

PART I: BONE DATING

Materials and Methods

Bone samples were pretreated as cremated bones for accelerator mass spectrometry (AMS) bioapatite dating (Van Strydonck et al. 2009). Infrared spectra were collected on KBr pellets of fresh and pretreated bone sample powder, using a Bruker Vertex 70 FTIR spectrometer (www.bruker.com), by accumulation of 16 scans with a resolution of 4 cm^{-1}.

These Fourier transform infrared spectroscopy (FTIR) spectra were used to evaluate the material properties of the bone: (1) the transformation of the bone mineral was evaluated by calculating the splitting factor (SF) of the ν_4 vibration mode of PO_4^{3-} between 495 and 750 cm^{-1} (FTIR-SF); and (2) the presence of cyanamide-apatite [$Ca_{10}(PO_4)_6CN_2$] or calcium deficient cyanamide-apatite [$Ca_9(PO_4)_5(HPO_4)(HCN_2)$] at ~2012 cm^{-1}, found frequently in cremated bone apatite and thought to be a possible indicator for the incineration of bones along with body tissues (skin, muscles, fat, etc.) (Hüls et al. 2010; Van Strydonck et al. 2010, 2013 and references therein).

Since bone samples could be interpreted as cremated/calcined bone material, radiocarbon dating was done on the carbonate fraction. Prepared bone material was hydrolyzed with H_3PO_4 to extract CO_2 graphitized for AMS ^{14}C measurement (Van Strydonck and van der Borg 1990–1991; Nadeau et al. 1998). Stable isotope composition ($\delta^{13}C$) was measured with a conventional mass spectrometer (IRMS, Finnigan-Mat-δ).

Results and Discussion

Samples from four individuals from different layers were ^{14}C dated (Table 1). The results show discrepancies between bone dates and the consensus value of the lime (see the next section). The dates confirm the observations made before (Van Strydonck et al. 2013) and show the possibility of a burial rite comprising a cremation of the bodies in the presence of rock carbonate powder. During cremation, fossil carbon, originating from the decomposition of calcium carbonate and the formation of quicklime, is built into the bioapatite structure. The carbon content of the bioapatite is rather constant in all four bones. No extreme values are observed in contradiction to what was observed on bones from urnfield cremation graves (minimum = 0.3 and maximum = 3.14‰ carbon).

Although sample pretreatment (e.g. strength of powdering) can slightly influence the FTIR-SF (Surovell and Stiner 2001), the measurements on pretreated bones still allow to differentiate between unburned bones (SF ~2.5–2.9) and well-calcined bones (SF ~7) (Stiner et al. 1995). The average SF from the Cova de Na Dent bones is 5.72 ± 1.23 with a minimum of 3.32 and a maximum of 8.10 (n = 43). This indicates, just as for the museum samples, that an important difference in the degree of incineration exists between the bones. This is caused by the heat absorption of the limestone during incineration (Van Strydonck et al. 2013). Visual inspection of the bones corroborates the important difference in degree of incineration (Figure 4).

Table 1 Radiocarbon results of bone samples.

Lab code	Layer	Bone	^{14}C age (BP)	Consensus value lime dating (BP)	$\Delta^{14}C$	Carbon (‰)	FTIR-SF
KIA-48309	0	lower limb	3935 ± 40	2883 ± 30	1052 ± 50	1.1	4.76 ± 0.52 (n = 3)
KIA-48306	1	femur	4155 ± 40	2746 ± 30	1409 ± 50	1.0	5.64 ± 0.02 (n = 2)
KIA-48308	1	skull	4765 ± 35	2746 ± 30	2019 ± 46	1.9	8.1 (n = 1)
KIA-48307	3	rib	4155 ± 40	1950 ± 30	2205 ± 50	1.5	5.64 ± 0.02 (n = 2)

Figure 4 White and black bones from layer −1

The presence of cyanamide-apatite or calcium-deficient cyanamide-apatite was recognized in the spectra of 12 bones out of 28 (Figure 5). All layers except layer 3 contained bones with an IR extinction band at ~2012 cm^{-1}. This may be a coincidence since only three bones of that layer were examined.

PART II: LIME ANALYSIS

Materials and Methods

Material Analysis of the Lime Conglomerate

Material analysis of the lime conglomerate is based on a combination of various analysis methods: petrographic analysis, X-ray diffraction crystallography (XRD), FTIR spectroscopy (FTIR), and simultaneous thermal analysis (STA).

Petrographic analysis of the lime conglomerate was performed by means of optical microscopy on a thin section with a Zeiss Axioplan microscope (www.zeiss.com) equipped with a DeltaPix digital camera (www.deltapix.dk), while X-ray diffraction crystallography was realized on a Bruker D8.

Simultaneous thermal analysis, consisting of a thermogravimetric analysis (TGA) coupled with differential scanning calorimetry (DSC), was carried out on a Netzsch STA 449 F3 Jupiter®. For that, approximately 30 to 45 mg of the size fraction below 100 μm of a manually crushed mortar sample was heated to 1200°C at a rate of 20°C/min. The weight loss between 200 and 600°C can be attributed to the loss of water chemically bound to hydraulic compounds and is therefore indicative for the hydraulicity of the binder fraction (Bakolas et al. 1998). At higher temperatures, in general up to 800°C, carbon dioxide is released from calcium carbonate, resulting in a significant weight loss.

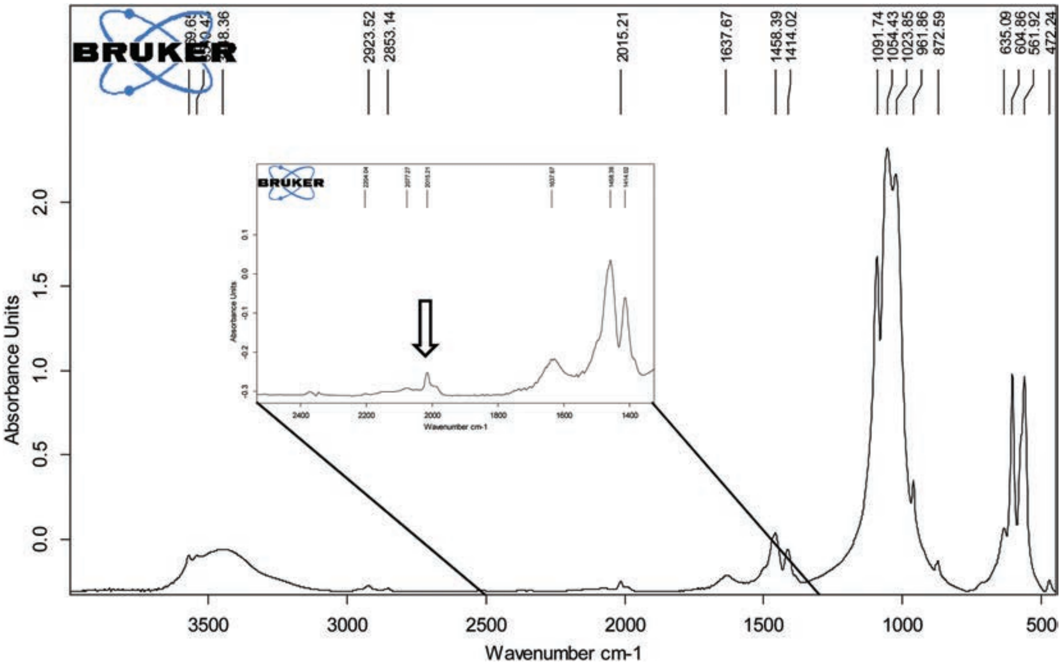

Figure 5 FTIR spectrum of a white bone (proximal phalanx M) from layer −1

Radiocarbon Dating

As suggested by analysis on museum objects (Van Strydonck et al. 2013), the burial ritual consisted of cremation of the body in contact with limestone. During this process, the limestone was burnt and transformed into quicklime (reaction [1]). After burial, the quicklime absorbed water [2] and hardened by the reaction with atmospheric CO_2 [3], a process termed carbonatation:

$$\text{Burning of rock carbonate: } CaCO_3\ (s) \xrightarrow{heat} CaO\ (s) + CO_2\ (g) \qquad [1]$$

$$\text{Slaking of quicklime: } CaO\ (s) \xrightarrow{water} Ca(OH)_2\ (s) \qquad [2]$$

$$\text{Hardening: } Ca(OH)_2\ (s) + CO_2\ (g) \xrightarrow{\quad} CaCO_3\ (s) + H_2O\ (l) \qquad [3]$$

Absorption of the atmospheric carbon dioxide enables the possibility for dating of the lime conglomerate and hence the lime burial rite. However, the possible presence of various carbonate sources, other than the carbonate formed during hardening, biases the $^{14}C/^{12}C$ isotopic ratio and hence interferes with the dating process. Common interfering sources of carbon are (i) fossil carbonates originating from unburnt residues of the limestone and (ii) secondary carbonatation deposits.

From a small lump of the lime burial, a sample was retrieved, being homogeneous in color and texture and not containing any bone material. The sample was dried, crushed, and sieved over a 250-µm sieve. Four successive CO_2 fractions were obtained by the titration method or sequential dissolution (Van Strydonck et al. 1982–1983, 2011). ^{14}C and stable isotope analyses were performed as described previously.

Results

Material Analysis of the Lime Conglomerate

The petrographic analysis of an incompletely burnt limestone fragment, retrieved from layer 2b, reveals information on the crushed limestone and hence on the source of the raw materials of the lime conglomerate. The limestone fragment is characterized by a calcinated rim of approximately 0.75–1 mm thickness, which gradually merges with the unburnt limestone deeper within. The limestone can be classified as crinoid biosparite, which has largely been recrystallized during diagenesis. However, the presence of crinoid columns can still easily be discerned in the thin section.

Petrographic analysis of one of the rare lime lumps found in the material shows that the limestone must have been crushed before use. The temperature and the time needed to decompose even a small limestone lump are too high and too long for a normal pyre using wood as fuel (Figure 6).

X-ray diffraction, FTIR spectroscopy and simultaneous thermal analyses all evidence that the lime conglomerate is composed mainly of calcium carbonate (Table 2, 90–95% $CaCO_3$ content). Based on the STA, the lime conglomerate can be identified as an almost pure putty lime. The only inorganic component in detectable quantities, besides calcium carbonate, has been sodium chloride (2–4%), most probably coming from the salty seawater.

Radiocarbon Dating

The ^{14}C results of the different fractions of each sample are represented in Table 3 and Figure 7. The consensus dates obtained by the extrapolation method (Van Strydonck et al. 2011) on the individual layers are consistent with the vertical stratigraphy (Figure 8). However, the results are not in agreement with the general archaeological conviction suggesting a date from the 5th century BC onwards, based on the presence of archaeological artifacts in previously excavated lime burials (Castro Martínez et al. 1997; Micó Pérez 2005, 2006). The results on Cova de Na Dent suggest an earlier start of this ritual. The youngest date from Cova de Na Dent (layer 3) is in accordance with the available data for the end of this ritual in the early Roman period. The presence of Roman pottery in the upper layers at the Son Matge lime burial as well as ^{14}C dates suggest that the site was in use until the 1st century AD (De Mulder and Van Strydonck 2012).

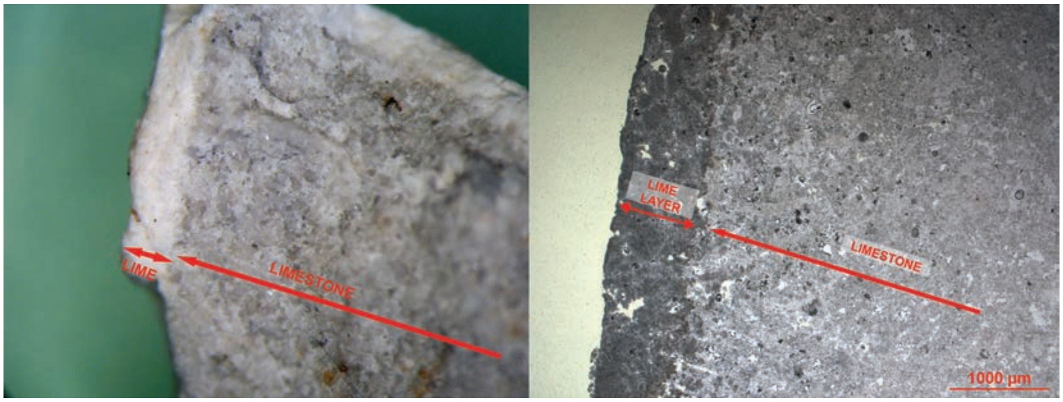

Figure 6 Light microscopic photograph of a section of a lime lump found in layer 2b. The cross-section of the lime lump (left) exhibits a white-colored outer layer, corresponding with the calcination rim of the limestone. In the thin-section micrograph (right), this layer is shown darker in color due to its higher density. Pores are died yellow because of the use of a colored impregnation resin, thus strongly influencing the color of porous material.

Table 2 Carbon and calcium carbonate content of the lime conglomerate as determined by the different analysis methods.

	Chemical analysis/X-ray diffraction		Simultaneous thermal analysis	
Layer	Carbon [wt%]	$CaCO_3$ [wt%]	Δw [600–1000°C] [wt%]	$CaCO_3$ [wt%]
3	11.22 ± 0.04	93.49 ± 0.33	42.50	96.65
2b	11.13 ± 0.15	92.74 ± 1.25	38.60	87.78
2a	11.09 ± 0.08	92.41 ± 0.67	41.48	94.33
1	11.25 ± 0.04	93.74 ± 0.33	42.03	95.59
0	10.99 ± 0.14	91.58 ± 1.17	41.27	93.86
−1	10.85 ± 0.03	90.41 ± 0.25	38.85	88.35

Unfortunately, the ^{14}C dates obtained on the lime conglomerate cannot be verified against ^{14}C dates or typochronological dates obtained on charcoal or artifacts, as these are completely absent within the Cova de Na Dent lime burial. Although the material analysis of the lime conglomerate suggests that it almost entirely consists of calcium carbonate, these analyses do not specify the nature of the carbonates. Especially the presence of fossil carbonates and secondary crystallization deposits could discord the ^{14}C-dating results of the lime burials. Hence, more detailed analysis is needed in order to identify the possible influence of these intervening sources. A first analysis has been performed based on the spread of the ^{14}C age between the different CO_2 fractions on a single layer and the results of a simultaneous thermal analysis of the layers.

Table 3 Radiocarbon dates from 4 fractions of a lime sample from each level.

Layer	Lab code (KIA-)	Fraction	% sample	^{14}C age (BP)	δ^{13}C ‰
−1	46085	1	18.08	2985 ± 30	−22.6
	46086	2	33.04	2920 ± 35	−23.6
	46087	3	23.82	2900 ± 30	−23.0
	46088	4	25.06	2855 ± 30	−22.9
0	46400	1	21.99	2870 ± 30	−21.2
	46401	2	27.52	2790 ± 30	−20.6
	46402	3	28.01	2760 ± 30	−20.4
	46403	4	22.48	2860 ± 25	−20.2
1	46378	1	31.59	2960 ± 30	−20.7
	46379	2	26.00	3350 ± 35	−21.5
	46380	3	24.88	3455 ± 30	−20.2
	46381	4	17.54	3530 ± 30	−19.4
2b	46975	1	24.09	3210 ± 30	−19.5
	46976	2	26.44	4035 ± 35	−22.3
	46977	3	29.38	4265 ± 30	−23.5
	46978	4	20.09	4315 ± 30	−23.7
2a	46971	1	23.44	2830 ± 25	−19.0
	46972	2	28.03	3365 ± 30	−21.2
	46973	3	33.22	3705 ± 30	−21.0
	46974	4	15.31	3830 ± 40	−21.0
3	46089	1	21.84	1985 ± 30	−17.7
	46090	2	20.66	2055 ± 35	−18.2
	46091	3	38.25	2135 ± 30	−15.1
	46092	4	19.24	2485 ± 30	−15.7

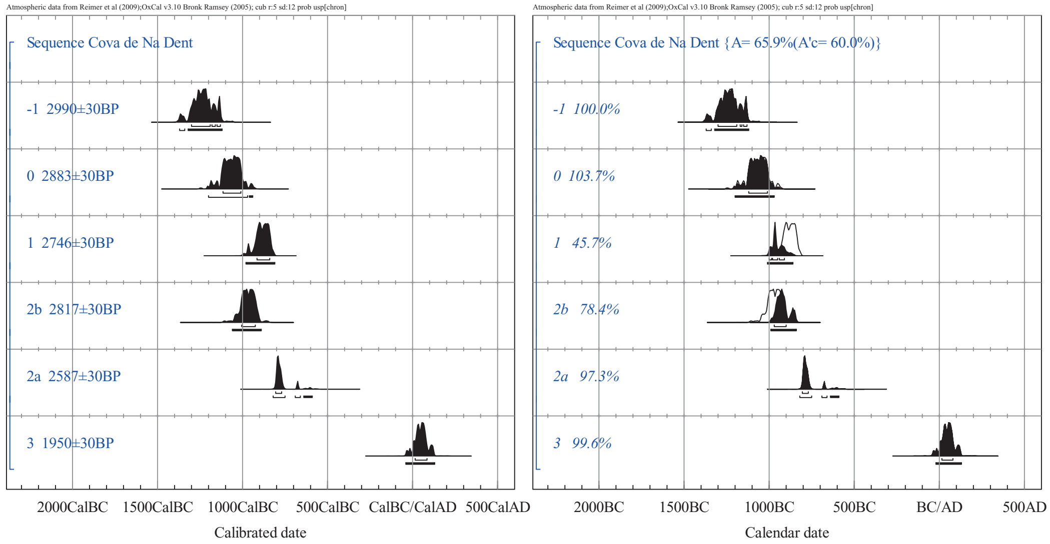

Figure 7 Consensus value for each layer before (left) and after (right) Bayesian analysis (OxCal v. 3.10, Bronk Ramsey 2009; atmospheric data from Reimer et al. 2009).

The different thermogravimetry (TG) curves (Figure 8), obtained on the individual layers, are all very similar. The only remarkable difference is the presence of a shoulder at higher temperatures (800~925°C range) adhered to the decarbonation cliff caused by the outgassing of carbon dioxide from the lime carbonate (600–800°C range). Based on the XRD analyses, the presence of mineral carbonate phases other than calcite can be excluded in amounts exceeding the detection limit of ~1–2 wt%. Especially the presence of dolomite, the most plausible alternative carbonate phase, can be excluded. As the thermal decomposition of dolomite [(Ca,Mg)CO_3] to $CaCO_3$, MgO, and CO_2 occurs at temperatures below the decomposition of $CaCO_3$, dolomite is (i) not present in amounts exceeding a few tenths of weight percent (Rowland and Beck 1952), and (ii) cannot be responsible for the weight losses observed at temperatures above 800°C. Other doped carbonates (containing for instance iron or strontium) have neither been identified by the XRD analyses and are therefore unlikely to being present in such amounts that they can be responsible for the weight losses observed at higher temperatures. The most likely explanation, therefore, is that the differences are due to crystallographic differences within the calcite as a result of their origin (fossil remains, anthropogenic formation, or from secondary carbonatation deposits).

The hypothesis is supported to some extent by the observations based on the spread of the ^{14}C ages of the different CO_2 fractions and stable isotope δ^{13}C (Table 4), taking into account, however, that the stable isotope shift can also be caused by diffusion effects (Van Strydonck et al. 1989). A significant spread on the ^{14}C ages of the CO_2 fractions correlates in most cases with the presence of a distinct calcination shoulder at higher temperatures. For example, based on the profile, layers −1 and 0 are supposed to contain the lowest amounts of fossil carbonates and minimal amounts of secondary carbonatation deposits. These layers exhibit an accordingly small shoulder in the TG curve. On the contrary, all other layers are supposed to contain both fossil carbonates and calcium carbonate originating from secondary carbonatation. With the exception of the sample collected from layer 2b, all of these are characterized by the presence of a distinct shoulder. In the case of layer 2b, the shoulder is present as well but definitely less pronounced as would be expected.

The differential scanning calorimetry (DSC) curves (Figure 8) exhibit for some of the layers also distinct characteristics. The double peak in the case of the sample collected from layer −1 is probably due to a read error as (i) the change occurs all of a sudden and (ii) the total measurement range of

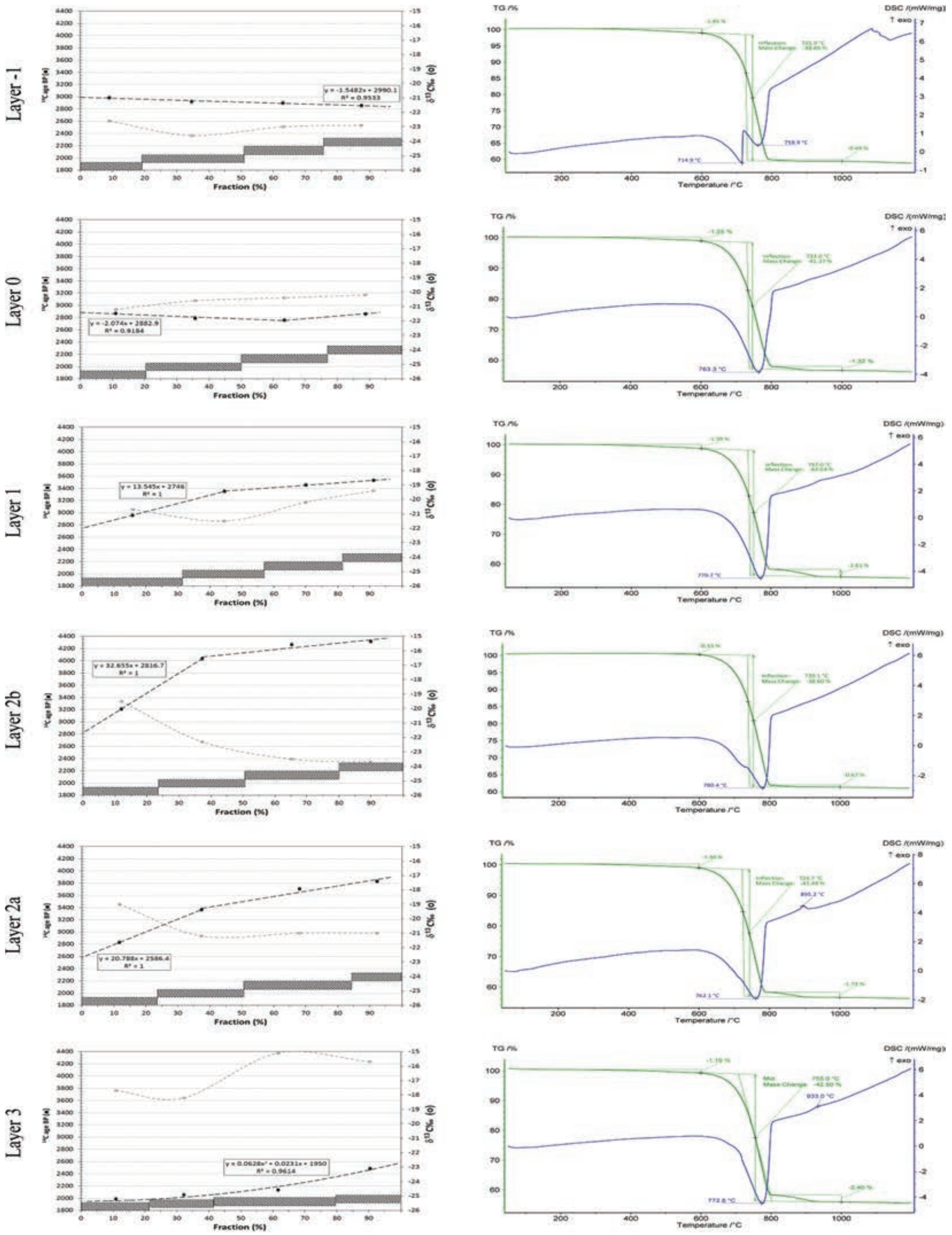

Figure 8 ^{14}C and stable isotope analysis (left) and STA (right) of the different fractions of 6 layers

Table 4 Maximal difference between the 4 fractions (Δ) of each layer.

Layer	−1	0	1	2b	2a	3
$\Delta\delta^{13}$C (‰)	1.0	1.0	2.1	4.2	2.2	3.1
Δ^{14}C (^{14}C yr)	130	110	570	1105	1000	500

the results corresponds more closely with the other results after correction. This change is therefore not considered any further. However, the DSC curves of the layers 1, 2a, and 3 exhibit a distinct bump at higher temperatures (~895°C in the case of sample 2a, less expressed and at a somewhat higher temperature in the case of samples 1 and 3). The origin of these bumps remains unclear.

While the material analyses of the lime conglomerate evidence that for each layer the conglomerate can be identified as almost pure lime putty, the nature of the carbonates is not readily specified. This, however, is known to influence the ^{14}C dating result as the presence of fossil carbonates and/or secondary carbonatation deposits will influence the ^{14}C ages of the separate CO_2 fractions. This in turn influences the interpretation and, hence, the determination of the ^{14}C age of the anthropogenic lime carbonate.

Analysis of the spread on the ^{14}C age between the different CO_2 fractions and the δ^{13}C isotopic profiles in combination with a simultaneous thermal analysis of each of the layers has identified the possible presence of a calcination shoulder at higher temperatures in the 800 ~925°C range in correspondence with the amount of fossil carbonates and/or secondary carbonatation deposits. However, a clear correlation with the findings based on the fractions cannot be found. It remains unclear whether the shoulder in the TG curve is effectively defined by the presence of fossil carbonates, secondary carbonatation products, or a combination of both, or whether the observations based on the stable isotope profiles are 100% correct or not.

Preliminary observations based on the petrographic analysis of thin sections, scanning electron microscopy (SEM), and optical cathodoluminescence microscopy on polished sections have, so far, not attributed additional evidence on this. However, a more detailed analysis is required to complete these preliminary findings.

GENERAL CONCLUSION

Aberrant ages of the bioapatite of the bones, showing ^{14}C depletion, the FTIR spectra as a proxy for crystallographic changes, as well as the general appearance of the bones, corroborate the idea of a burial rite comprising a cremation of the bodies in the presence of fine crushed rock carbonate. These effects are detectable on bones from old museum collections as well on freshly excavated material. Altering of the bones due to decades of storage in not acclimatized museum storage can be ruled out.

The ^{14}C dates of Cova de Na Dent support an earlier chronology as generally accepted (Micó Pérez 2005, 2006). Because of the absence of artifacts in Cova de Na Dent, the apparent disagreement between the traditional typochronology and the ^{14}C chronology cannot be solved. However, an earlier chronology is supported by the data from the Son Matge lime burial (Van Strydonck and Waldren 1990, 1995). Furthermore, the correlation between the ^{14}C and TGA analyses suggest that the lowest layer (−1) of the lime burial is almost free of contaminating carbonates. The date obtained for this layer should thus be acceptable. However, further research is needed to complete the correlation between the TGA results and the presence and amount of contaminants.

REFERENCES

Bakolas A, Biscontin G, Moropoulou A, Zendri E. 1998. Characterization of structural Byzantine mortars by thermogravimetric analysis. *Thermochimica Acta* 321(1–2):151–60.

Bronk Ramsey C. 2009. Bayesian analysis of radiocarbon dates. *Radiocarbon* 51(1):337–60.

Castro Martínez PV, Gili Suriñach S, González Marcén P, Lull V, Micó Perez R, Rihuete Herrada C. 1997. Radiocarbon dating and the Prehistory of the Balearic Islands. *Proceedings of the Prehistoric Society* 63:55–86.

De Mulder G, Van Strydonck M. 2012. Un descubrimiento imprevisto. Nuevos hallazgos de ceramic en Son Matge. *Bolletí de la Societat Arqueològica Lulliana* 68:15–25.

Hüls CM, Erlenkeuser H, Nadeau M-J, Grootes PM, Andersen N. 2010. Experimental study on the origin of cremated bone apatite carbon. *Radiocarbon* 52(2):587–99.

Micó Pérez R. 2005. *Cronologià absoluta y periodización de la prehistoria de las Islas Baleares*. BAR International Series 1373. Oxford: Tempus Reparatum. 621 p.

Micó Pérez R. 2006. Radiocarbon dating and Balearic prehistory: reviewing the periodization of the prehistoric sequence. *Radiocarbon* 48(3):421–4.

Nadeau M-J, Grootes PM, Schliecher M, Hasselberg P, Rieck A, Bitterling M. 1998. Sample throughput and data quality at the Leibniz-Labor AMS facility. *Radiocarbon* 40(1):239–45.

Reimer PJ, Baillie MGL, Bard E, Bayliss A, Beck JW, Blackwell PG, Bronk Ramsey C, Buck CE, Burr GS, Edwards RL, Friedrich M, Grootes PM, Guilderson TP, Hajdas I, Heaton TJ, Hogg AG, Hughen KA, Kaiser KF, Kromer B, McCormac FG, Manning SW, Reimer RW, Richards DA, Southon JR, Talamo S, Turney CSM, van der Plicht J, Weyhenmeyer CE. 2009. IntCal09 and Marine09 radiocarbon age calibration curves, 0–50,000 years cal BP. *Radiocarbon* 51(4):1111–50.

Rowland RA, Beck CW. 1952. Determination of small quantities of dolomite by differential thermal analysis. *American Mineralogist* 37:76–82.

Stiner MC, Kuhn SL, Weiner S, Bar-Yosef O. 1995. Differential burning, recrystallization, and fragmentation of archaeological bone. *Journal of Archaeological Science* 22(2):223–37.

Surovell TA, Stiner MC. 2001. Standardizing infra-red measures of bone mineral crystallinity: an experimental approach. *Journal of Archaeological Science* 28(6):663–42.

Van Strydonck M, van der Borg K. 1990–1991. The construction of a preparation line for AMS-targets at the Royal Institute for Cultural Heritage Brussels. *Bulletin of the Royal Institute for Cultural Heritage* 23:228–34.

Van Strydonck M, Waldren WH. 1990. Radiocarbon dating of lime burials. In: Mook WG, Waterbolk HT, editors. Proceedings of the Second International Symposium ^{14}C and Archaeology Groningen, 1987. *PACT* 29:403–14.

Van Strydonck M, Waldren WH. 1995. Radiocarbon dating of the Son Matge rock shelter. In: Waldren WH, Ensenyat JA, Kennard RC, editors. *Ritual, Rites and Religion in Prehistory. IIIrd Deya International Conference of Prehistory*. BAR International Series 611, Volume I. Oxford: Tempus Reparatum. p 164–82.

Van Strydonck M, Dupas M, Dauchot-Dehon M, Pachiaudi C, Maréchal J. 1982–1983. A further step in the radiocarbon dating of old mortars. *Bulletin of the Royal Institute for Cultural Heritage* 19:155–71.

Van Strydonck M, Dupas M, Keppens E. 1989. Isotopic fractionation of oxygen and carbon in lime mortar under natural environmental conditions. *Radiocarbon* 31(3):610–8.

Van Strydonck M, Boudin M, De Mulder G. 2009. ^{14}C dating of cremated bones: the issue of sample contamination. *Radiocarbon* 51(2):553–68.

Van Strydonck M, Boudin M, De Mulder G. 2010. The carbon origin of structural carbonate in bone apatite of cremated bones. *Radiocarbon* 52(2):578–86.

Van Strydonck M, Boudin M, Decq L, Van den Brande T, Borms H, Ramis D, De Mulder G. 2011. AMS ^{14}C dating of Balearic lime burials. *Radiocarbon* 53(4):563–74.

Van Strydonck M, Decq L, Van den Brande T, Boudin M, Ramis D, Borms H, De Mulder G. 2013. The protohistoric 'quicklime burials' from the Balearic Islands: cremation or inhumation. *Osteoarchaeology*. doi: 10.1002/oa.2307.

Waldren WH, Van Strydonck M. 1995. Deed or murder most foul? Ritual, rite or religion? Mallorca inhumation in quicklime. In: Waldren WH, Ensenyat JA, Kennard RC, editors. *Ritual, Rites and Religion in Prehistory. IIIrd Deya International Conference of Prehistory*. BAR International Series 611, Volume I. Oxford: Tempus Reparatum. p 146–63.